ELSEVIER

Journal of Organometallic Chemistry 629 (2001) 165–170

Journal of Organometallic Chemistry

www.elsevier.com/locate/jorganchem

A novel dimanganese complex linked by an unusually strong hydrogen bond. X-ray structure of the hydrogen-bonded complex and ab initio calculations

Thomas M. Becker [a], Jeanette A. Krause Bauer [a], Janet E. Del Bene [b], Milton Orchin [a,*]

[a] *Department of Chemistry, University of Cincinnati, PO Box 210172, Cincinnati, OH 45211-0172, USA*
[b] *Department of Chemistry, Youngstown State University, Youngstown, OH 44555, USA*

Received 23 January 2001; received in revised form 3 April 2001; accepted 8 April 2001

Abstract

In an attempt to prepare the fluoro complex $(CO)_3$(dppe)MnF (**3**) by treating a CH_2Cl_2 solution of the aqua complex $[(CO)_3(dppe)Mn(OH_2)]BF_4$ (**1**) with $NaF_{(aq)}$, we isolated instead, the dimanganese complex, $[(CO)_3(dppe)Mn(OH_2)\cdots FMn(dppe)(CO)_3]BF_4$ (**2**). The two moieties, **1** and **3**, are held together by an unusually strong O–H···F hydrogen bond (O···F = 2.458(3) Å, H···F = 1.52 Å) between the aqua ligand on one manganese and the fluoro atom on the other manganese. Using as a simple model the interaction between $^+Li(H_2O)$ and FLi, the hydrogen bonding distance O–H···F was calculated to be; O···F = 2.443 Å. Authentic **3** was prepared in a homogeneous system using CH_2Cl_2-soluble $[Et_4N]F$.

Keywords: Dimanganese complexes; Strong hydrogen bonds; X-ray structures; ab initio

1. Introduction

The readily available Mn–aqua complex, $[(CO)_3(dppe)Mn(OH_2)]BF_4$ (**1**), has proven extremely useful for the preparation of a great variety of functional groups sigma bonded to the Mn center [1,2]. The utility of this complex relies on the lability of the aqua ligand and its ease of replacement by either neutral or anionic ligands. Anionic ligands that have been used include OMe, OC(O)OMe, O(Tf), NO_3, Cl, Br, CN and N_3. The usual procedure for the reaction involves dissolving the aqua complex in CH_2Cl_2 and adding an excess of a concentrated aqueous solution of the sodium salt of the desired anion, separating the phases, and isolation of the desired complex from the CH_2Cl_2 solution. When this procedure was followed in an attempt to prepare the fluoro complex, we isolated a crystalline compound whose unexpected structure proved to be that shown in Fig. 1.

2. Experimental

All reactions were carried out under an argon atmosphere unless otherwise noted. Solvents were used as received. 1,2-Bis(diphenylphosphino)ethane (dppe) was purchased from Pressure Chemicals. The aqua complex [*fac*-$Mn(CO)_3$(dppe)$(OH_2)]BF_4$ (**1**) was prepared according to the literature method [1]. Tetraethylammonium fluoride hydrate was purchased from Aldrich. IR spectra were recorded on a P-E Spectrum One FT-IR employing 1.0 mm NaCl liquid cells. ^{1}H-NMR spectra were obtained on $CDCl_3$ solutions using a Bruker AC-250 spectrometer with chemical shifts recorded relative to Me_4Si. Q-Tof hybrid quadrupole time of flight

* Corresponding author. Tel.: +1-513-5569200; fax: +1-513-5569239.
E-mail address: orchinm@email.uc.edu (M. Orchin).

0022-328X/01/$ - see front matter
PII: S0022-328X(01)00829-4

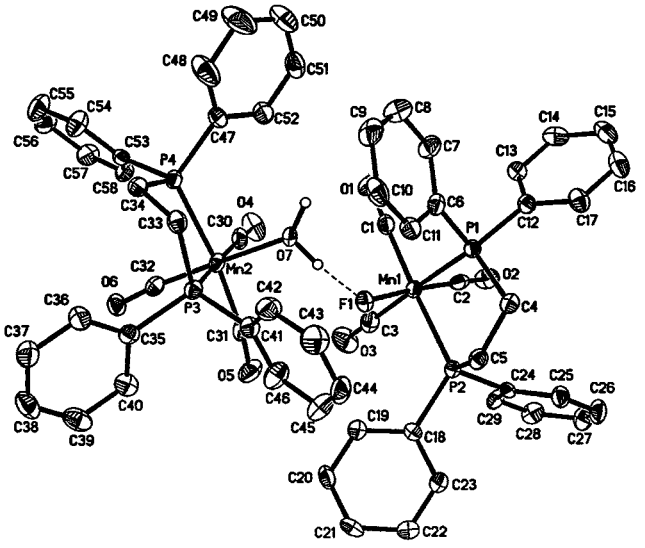

Fig. 1. ORTEP diagram of $[(CO)_3(dppe)Mn(OH_2)\cdots FMn(dppe)(CO)_3]BF_4$ (**2**) indicating labeling scheme and 50% thermal ellipsoids. The BF_4 counterion and the external H_2O, which crystallizes in the lattice, are not shown.

mass spectrometer (Micromas UK Ltd.) fitted with an electrospray ionization (ESI) was used for the analysis of the compounds. Melting points were determined using a Mel-Temp apparatus and they are uncorrected. Chemisar Laboratories performed elemental analyses.

2.1. Preparation of $[(CO)_3(dppe)Mn(OH_2)\cdots FMn(dppe)(CO)_3]BF_4$ (2)

A solution of the aqua complex **1** (0.107 g, 0.167 mmol) in ca. 25 ml of CH_2Cl_2, was placed in a round bottomed flask. Excess $NaF_{(aq)}$ (0.080 g, 1.91 mmol, in 1 ml of H_2O) was added and the two-phase reaction mixture was stirred for 2.5 h. The CH_2Cl_2 solution was separated, then washed with water (2×5 ml). After concentration, hexane was added and after cooling in the refrigerator, yellow X-ray quality crystals of **2** were isolated.

Data **2**: m.p. 171–174°C. IR (cm^{-1}, CH_2Cl_2): $\nu(OH)_{anti}$ 3682.1, $\nu(OH)_{sym}$ 3602.9, $\nu(CO)$ 2037 s, 2025 s, 1964 s, 1950 s, 1938 s, 1916 s. ^{1}H-NMR (δ, $CDCl_3$) 7.67–7.04 (m, Ph, 40H), 3.0–2.0 (m, CH_2, H_2O, 10H). MS (m/z) 537 $Mn(dppe)(CO)_3^+$, 453 $Mn(dppe)^+$. Anal. Calc. for $C_{58}H_{52}BF_5Mn_2O_8P_4$: C, 57.26; H, 4.30. Found: C, 56.97; H 3.82%.

2.2. Preparation of $(CO)_3(dppe)MnF$ (3)

2.2.1. From $[fac\text{-}Mn(CO)_3(dppe)(OH_2)]BF_4$ (1)

A solution of the aqua complex **1** (0.297 g, 0.463 mmol) in ca. 25 ml of CH_2Cl_2 was placed in a round bottomed flask. Excess $[NEt_4]F\cdot xH_2O$ (0.277 g) was added and the one phase system was stirred for 25 min. The CH_2Cl_2 solution was washed with water (4×10 ml) and the CH_2Cl_2 was removed by rotary evaporation. The yellow residue was dissolved in benzene and filtered to remove remaining $[NEt_4]F$. The benzene was removed via rotary evaporation leaving the yellow solid **3**. The IR spectrum of **3** in CH_2Cl_2 must be taken immediately after the solution is placed in the IR cell to avoid reaction with the NaCl cell (see section 2.7).

The one-phase system using CH_2Cl_2-soluble $[NEt_4]F$ as the fluoride source in the reaction with **1** is the preferred procedure for preparing the fluoro complex **3**. The use of a two-phase system involving a CH_2Cl_2 solution of the aqua complex and NaF in an attempt to synthesize **3** instead leads to **2** as described in Section 2.1. Reversing the order of addition by slowly dripping **1** into $NaF_{(aq)}$ did not change the result.

Data **3**: mp 146–150°C. IR (cm^{-1}, CH_2Cl_2): ν(CO) 2024s, 1948s, 1907s. ^{1}H-NMR (δ, $CDCl_3$) 7.75–7.25 (m, Ph, 20H), 2.79–2.73 (m, CH_2, 4H). High Res. MS (m/z) 537.0558 $Mn(dppe)(CO)_3^+$ (Calc. 537.0581), 472.0743 $Mn(dppe)F^+$ (Calc. 472.0718), 453.0739 $Mn(dppe)^+$ (Calc. 453.0734).

2.2.2. From $[(CO)_3(dppe)Mn(OH_2)\cdots FMn(dppe)(CO)_3]BF_4$ (2)

A solution of the hydrogen-bonded dimanganese complex **2** (23 mg, 0.019 mmol) in ca. 15 ml of CH_2Cl_2. was placed in a round bottomed flask. Excess $[NEt_4]F\cdot xH_2O$ (35 mg) was added and the homogeneous system was stirred for 3 h. The CH_2Cl_2 solution was separated, washed with water (2×10 ml) and then concentrated. Hexane was added and the solution was cooled. The precipitated yellow fluoro complex $(CO)_3$(dppe)MnF (**3**) was then collected.

2.3. Reaction of $[(CO)_3(dppe)Mn(OH_2)\cdots FMn(dppe)(CO)_3]BF_4$ (2) with CO

A small quantity of the hydrogen-bonded dimanganese complex **2** ($\sim$20 mg) was added to a round bottomed flask and dissolved in ca. 15 ml of CH_2Cl_2. CO was bubbled into the solution for 1 min, the flask was stoppered and the solution was stirred for 3 h. The TLC and the IR spectrum of the solution taken quickly indicated the presence of a mixture of the known tetracarbonyl complex $[(CO)_4Mn(dppe)]BF_4$ [3] and the fluoro complex **3**.

2.4. Reaction of $(CO)_3(dppe)MnF$ (3) with NaCl

When a CH_2Cl_2 solution of **3** is placed in the NaCl IR cell, the carbonyl stretching bands, originally observed, shift during ca. 5 min, to give final frequencies

Table 1
Selected bond lengths (Å) and bond angles (°) for $[(CO)_3(dppe)Mn(OH_2)\cdots FMn(dppe)(CO)_3]BF_4$ (**2**)

Details involving the F···H–O hydrogen-bonded interaction			
O(7)–H(1)	0.91	Mn(1)···O(7)	3.930
O(7)–H(2)	0.95	H(1)···F(1)	1.52
O(7)···F(1)	2.458(3)	O(7)–H(1)···F(1)	166
H(1)–O(7)–H(2)	110	H(2)–O(7)–Mn(2)	126
Mn(1)–F(1)–H(1)	127	Mn(1)–F(1)···O(7)	122
General bonding details			
Mn(1)–C(2)	1.783(4)	Mn(1)–C(3)	1.842(5)
Mn(1)–C(1)	1.843(4)	Mn(1)–F(1)	2.028(2)
Mn(1)–P(2)	2.3400(12)	Mn(1)–P(1)	2.3482(12)
O(1)–C(1)	1.144(5)	O(2)–C(2)	1.160(5)
O(3)–C(3)	1.146(5)	Mn(2)–C(32)	1.784(4)
Mn(2)–C(31)	1.820(5)	Mn(2)–C(30)	1.837(5)
Mn(2)–O(7)	2.072(3)	Mn(2)–P(4)	2.3434(12)
Mn(2)–P(3)	2.3511(12)	O(4)–C(30)	1.148(5)
O(5)–C(31)	1.146(5)	O(6)–C(32)	1.157(4)
Bond angles			
C(2)–Mn(1)–C(3)	89.7(2)	C(2)–Mn(1)–C(1)	91.0(2)
C(3)–Mn(1)–C(1)	92.3(2)	C(2)–Mn(1)–F(1)	174.26(14)
C(3)–Mn(1)–F(1)	93.5(2)	C(1)–Mn(1)–F(1)	93.61(14)
C(2)–Mn(1)–P(2)	92.29(12)	C(3)–Mn(1)–P(2)	93.42(14)
C(1)–Mn(1)–P(2)	173.41(13)	F(1)–Mn(1)–P(2)	82.78(7)
C(2)–Mn(1)–P(1)	92.99(13)	C(3)–Mn(1)–P(1)	176.18(14)
C(1)–Mn(1)–P(1)	90.35(13)	F(1)–Mn(1)–P(1)	83.59(7)
P(2)–Mn(1)–P(1)	83.79(4)	C(32)–Mn(2)–C(31)	84.5(2)
C(32)–Mn(2)–C(30)	93.7(2)	C(31)–Mn(2)–C(30)	88.8(2)
C(32)–Mn(2)–O(7)	174.2(2)	C(31)–Mn(2)–O(7)	96.08(14)
C(30)–Mn(2)–O(7)	92.13(14)	C(32)–Mn(2)–P(4)	88.49(13)
C(31)–Mn(2)–P(4)	172.53(13)	C(30)–Mn(2)–P(4)	94.27(14)
O(7)–Mn(2)–P(4)	90.60(8)	C(32)–Mn(2)–P(3)	92.34(13)
C(31)–Mn(2)–P(3)	93.74(14)	C(30)–Mn(2)–P(3)	173.64(13)
O(7)–Mn(2)–P(3)	81.82(8)	P(4)–Mn(2)–P(3)	83.87(4)

consistent with the previously reported chloro complex $(CO)_3$(dppe)MnCl (**4**) [4]. To verify that the fluoride in **3** converts to chloride **4** while in the IR cell, a small quantity of **3** ($\sim$20 mg) was dissolved in a minimal amount of CH_2Cl_2 and excess $NaCl_{(aq)}$ was added. The mixture was stirred overnight. An IR spectrum taken immediately after the solution was placed in the cell and monitored over the course of about 5 min, indicated that the fluoro complex **3** (2024, 1948, 1907 ν(CO) cm^{-1}) was completely converted into the chloro complex **4** (2025, 1955, 1914 ν(CO) cm^{-1}).

2.5. X-ray structure of 2

Single crystals of **2**, $[C_{58}H_{50}FO_7P_4Mn_2]BF_4.H_2O$, were obtained as pale yellow blocks from CH_2Cl_2/hexane. Crystal data: $M = 1216.57$, triclinic, $a = 10.655(2)$, $b = 15.714(3)$, $c = 17.745(2)$ Å, $\alpha = 74.620(6)$, $\beta = 80.021(8)$, $\gamma = 84.205(8)°$, $V = 2816.6(7)$ Å^3, space group $P\bar{1}$, $Z = 2$, $D_{calc} = 1.434$ Mg m^{-3}, $\mu = 0.532$ mm^{-1}. A crystal with dimensions of $0.10 \times 0.10 \times 0.10$ mm was mounted on a glass fiber with epoxy resin, intensity data were collected at 150 K on a SMART 1 K CCD diffractometer [5], graphite-monochromated Mo–K_a radiation, $\lambda = 0.71073$ Å, detector distance of 5.083 cm, θ range 2.41–28.21° with limiting indices of $-13 < h < 14$, $-20 < k < 20$, $-23 < l < 23$; 29 577 reflections collected of which 13 475 are independent reflections ($R_{int} = 0.0950$). Data corrections were applied using SADABS [6].

The structure was solved by direct methods using SHELXTL v5.03 [7] and refined by full-matrix least-squares on F^2. Non-hydrogen atoms were refined with anisotropic displacement parameters. O–H hydrogens were held fixed where located, all other hydrogens were treated with a riding model, isotropic temperature factors were defined as $a*U_{eq}$ of the adjacent atom ($a = 1.5$ for OH and 1.2 for all others). Final $R_1 = 0.0619$, $wR_2 = 0.1035$ for 7038 reflections [$I > 2\sigma(I)$] and 703 parameters ($R_1 = 0.1501$, $wR_2 = 0.1308$ for all data). A final difference Fourier map was featureless, with the highest residual electron density peak of 0.568 e Å^{-3}. Selected bond lengths (Å) and angles (°) for $[(CO)_3(dppe)Mn(OH_2)\cdots FMn(dppe)(CO)_3]BF_4$ (**2**) are shown in Table 1.

2.6. Hydrogen-bonding model and ab initio calculations

We have used the hydrogen-bonded cationic complex $Li^+(H_2O)$:FLi as a model for that part of the structure of **2** which exhibits an $Mn^+(H_2O)$:FMn hydrogen bond. The structures of this model complex and the corresponding monomers $Li^+(H_2O)$ and FLi were geometry optimized with electron correlation effects included at second-order Møller–Plesset perturbation theory [MBPT(2) = MP2] [8–11] with the 6-31 + G(d,p) basis set [12–15], a valence double-split basis with polarization functions on all atoms and diffuse functions on all non-hydrogen atoms. This level of theory has been shown to yield structures of hydrogen-bonded complexes in agreement with experimental structures [16]. Harmonic vibrational frequencies were computed to confirm that the complex and monomers are equilibrium structures on their respective potential surfaces, and to evaluate zero-point vibrational energy contributions to the binding enthalpy at 0 K ($\Delta H°$). The electronic binding energy (ΔE_e) has been computed as the energy for the reaction:

$$Li^+(H_2O) + FLi \rightarrow Li^+(H_2O):FLi \quad (1)$$

For improved energetics, these calculations were carried out at MP2 with the Dunning correlation-consistent polarized valence triple-split basis set augmented with diffuse functions on non-hydrogen atoms (aug′-cc-pVTZ) [17–19]. For all calculations electrons below the valence shells were frozen in the Hartree–Fock 1s orbitals. These calculations were carried out using GAUSSIAN-98 [20] on the SGI-Origin computer at the Ohio Supercomputer Center.

3. Results and discussion

The aqua complex *fac*-[$(CO)_3$(dppe)Mn(OH_2)]BF_4 (**1**) is a relatively thermodynamically stable complex but it reacts rapidly with almost any anionic species to form neutral complexes in which the site originally occupied by the aqua ligand is taken up by the anion. We first became aware of this fact when we discovered that during the time required to take the infrared spectrum of a CH_2Cl_2 solution of this complex in a NaCl cell, rapid conversion to the corresponding chloro complex, *fac*-$(CO)_3$(dppe)MnCl (**4**) occurred [1]. The small quantity of adventitious water present in the solvent apparently dissolved sufficient NaCl to cause the reaction. We subsequently prepared authentic chloride by treating a CH_2Cl_2 solution of the aqua complex with an aqueous solution of NaCl [4]. In applying a similar procedure for the preparation of the fluoro complex, $(CO)_3$(dppe)MnF (**3**), we isolated instead, as detailed in Section 2.1, the rather unusual hydrogen-bonded dimanganese complex (**2**) possessing the structure shown in Fig. 1.

3.1. Reactions of [$(CO)_3$(dppe)Mn(OH_2)···FMn(dppe)$(CO)_3$]BF_4 (2) and $(CO)_3$(dppe)MnF (3) with Cl^- of the NaCl infrared cell

In attempting to determine the IR spectrum of **2** in CH_2Cl_2 solution, using a NaCl cell, we observed a change in spectrum with time, quite similar to the same phenomenon encountered while taking the spectrum of the aqua complex **1** as discussed above. If the aqua ligand in the hydrogen-bonded complex **2** were displaced by chloride (provided by the infrared cell) with concurrent splitting of **2**, one might expect a mixture of the resulting chloro and fluoro complexes. If, in addition, the fluoro ligand in the fluoro complex were very labile then this complex might also be converted to the chloro complex. In fact this turns out to be the case. When a CH_2Cl_2 solution of authentic **3** was placed in the NaCl cell, the change in spectrum demonstrated that the fluoro complex was completely transformed to the corresponding chloro complex in about 5 min (see section Section 2.4). It is indeed surprising that such fluoride–chloride exchange is so facile. It may be that F^- removal is facilitated by traces of H_2O.

3.2. Reaction of [$(CO)_3$(dppe)Mn(OH_2)···FMn(dppe)$(CO)_3$]BF_4 (2) with CO

We have shown previously [21] that when the aqua complex **1** is treated with CO, the aqua ligand is readily replaced to give the tetracarbonyl complex [$(CO)_4$-(dppe)Mn]BF_4. When the hydrogen-bonded complex **2** is treated similarly, the same tetracarbonyl complex is formed (IR) along with the fluoro complex **3**. This indicates cleavage of complex **2** during the reaction. The reaction was not further investigated.

3.3. Molecular structure of [$(CO)_3$(dppe)Mn(OH_2)···FMn(dppe)$(CO)_3$]BF_4 (2)

Complex **2** consists of $(CO)_3$(dppe)Mn(OH_2) and $(CO)_3$(dppe)MnF moieties held together by an O–H···F hydrogen-bond. Although the crystal structure of **2** also contains a BF_4 counterion and an external H_2O molecule, these are not shown in Fig. 1. The $(CO)_3$(dppe)MnF moiety is structurally similar to the chloro complexes, $(CO)_3$(P–P)MnCl (P–P = dppe, **4** [22], depe [23] and dppp [24]) in that the Mn is octahedrally coordinated with the F, three carbonyls, and the diphosphine occupying the six bonding sites. The Mn–F distance of 2.028(2) Å in **2** is longer than that commonly observed for M–F bonds [25], however, a similar lengthening of the M–F bond is observed for the M–FHF unit in *trans*-$Ru(dmpe)_2(H)(FHF)$, 2.284 Å [26] and $Mo(PMe_3)_4(F)(FHF)$, 2.124 Å [27].

The geometry about the Mn atom in the $(CO)_3$(dppe)Mn(OH_2) moiety is octahedral with an OH_2 molecule occupying one of the coordination sites on the metal. The Mn–O distance, 2.072(3) Å, is consistent with the bond distance reported for the triclinic form of **1** [28], 2.075(2) Å, the monoclinic form of **1** [1], 2.102(3) Å, and for [(depe)$(CO)_3$Mn(OH_2)]BF_4 [1], 2.115(2) Å. The triclinic structure of **1** crystallizes with one external molecule of H_2O.

The most striking structural feature of **2** is the very short O–H···F hydrogen-bond distance observed for the cation, O(7)···F(1) = 2.458(3) Å, H(1)···F(1) = 1.52 Å and O(7)–H(1)···F(1) = 166°. In contrast, the O–H···F interaction between the BF_4 counterion and the external H_2O is substantially longer (O(8)···F(4) = 2.864(4) Å, H(3)···F(4) = 1.93 Å, 172° and O(8)···F(3) = 3.018(5) Å, H(4)···F(3) = 2.17 Å, 149°). Long O–H···F interactions (O···F = 2.68–3.66 Å, H···F = 1.80–2.67 Å and angles at H of 104–174°) were also observed in monoclinic **1** [1] and triclinic **1** [28] between the aqua ligand and the BF_4 counterion and also between the BF_4 and the external H_2O in triclinic **1**. In a recent review by Steiner [29], hydrogen-bond distances to halide ions for organic and organometallic structures were found to have mean O···F^- and H···F^- distances of 2.68 and 1.71 Å (angles at H > 140°) for H–O–H donors, this represents the weakest interaction. Hydrogen-bond interactions with donors (D) such as C–O–H are stronger (mean D···F^- and H···F^- = 2.57, 1.58 Å) and the strongest are O–H donors (mean D···F^- and H···F^- = 2.47, 1.50 Å) which are bonded to the atoms N, P and As.

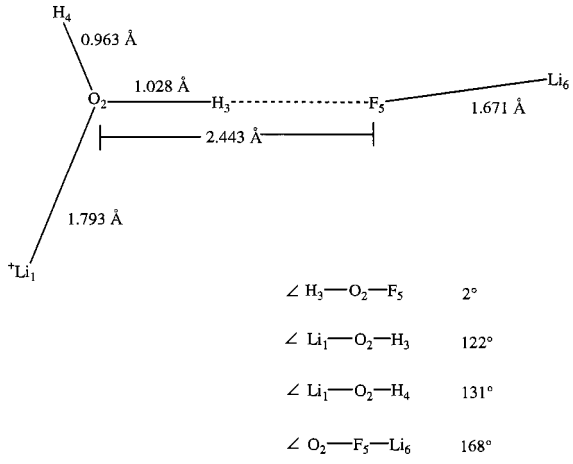

Fig. 2. Calculated bond angles and bond distance for $Li^+(H_2O)$: FLi.

To gain further insight of this rather unusual bonding motif, we have examined the model complex $Li^+(H_2O)$:FLi, in which Mn(1) (Fig. 1) has been replaced by Li, and Mn(2) (Fig. 1) by Li^+. The optimized structure of this model complex (see Fig. 2) has features that are quite similar to those observed experimentally for **2**. When Li^+ is bonded to one H_2O molecule, the hydrated ion Li^+:H_2O has C_{2v} symmetry, with Li^+ positioned at the negative end of the water dipole moment vector. Thus, this species is stabilized by strong electrostatic attractions. In the model complex $Li^+(H_2O)$:FLi, Li^+ is similarly bonded to the oxygen. Because the proton-donor in the model complex is a cationic species, the O···F distance is very short, at 2.443 Å, and the O–H···F hydrogen bond is essentially linear. In addition, the O–F–Li angle is very large at 168°. This orientation does not provide the best orientation for a directed lone pair on F participating in the hydrogen bond. Rather, in small cationic complexes the orientation of the proton acceptor molecule tends to favor a head-to-tail alignment of the bond dipole moment of the proton donor ion with the dipole moment of the proton acceptor molecule. In the model complex, the hydrogen bonded O–H bond of water is lengthened considerably, from 0.968Å in $Li^+(H_2O)$ to 1.028 Å in $Li^+(H_2O)$:FLi. All of these structural characteristics are consistent with the presence of a very strong O–H···F hydrogen bond, which has a computed MP2/aug'-cc-pVTZ binding energy (ΔE_e) of -38.7 kcal mol^{-1}, and a binding enthalpy ($\Delta H°$) of -37.6 kcal mol^{-1}.

4. Supplementary material

Crystallographic data (excluding structure factors) for the structural analysis have been deposited with the Cambridge Crystallographic Data Centre, CCDC no. 156936. Copies of this information may be obtained from The Director, CCDC, 12 Union Road, Cambridge CB2 1EZ, UK (fax: +44-1233-336-033; e-mail: deposit@ccdc.cam.ac.uk or www: http://www.ccdc.cam.ac.uk). Structure factors are available upon request from the authors.

Acknowledgements

CCD data was collected through the Ohio Crystallographic Consortium, funded by the Ohio Board of Regents 1995 Investment Fund (CAP-075) located at the University of Toledo, Instrumentation Center in A&S, Toledo, OH 43606.

References

[1] T.M. Becker, J.A. Krause Bauer, C. Homrighausen, M. Orchin, Polyhedron 18 (1999) 2563.
[2] T.M. Becker, J.A. Krause Bauer, C. Homrighausen, M. Orchin, J. Organomet. Chem. 602 (2000) 97.
[3] M. Orchin, S.K. Mandal, J. Feldman, Inorg. Synth. 32 (1998) 298.
[4] G.Q. Li, J. Feldman, J.A. Krause, M. Orchin, Polyhedron 16 (1997) 2041.
[5] SMART v5.054 and SAINT v5.A06 programs were used for data collection and data processing, respectively, Siemens Analytical X-ray Instruments Inc., Madison, WI.
[6] G.M. Sheldrick, SADABS was used for the application of semi-empirical absorption and beam corrections, University of Göttingen, Germany, 1996.
[7] G.M. Sheldrick, SHELXTL v5.03 was used for the structure solution and generation of figures and tables as well as neutral-atom scattering factors, University of Goettingen, Germany and Siemens Analytical X-ray Instruments Inc., Madison, WI.
[8] J.A. Pople, J.S. Binkley, R. Seeger, Int. J. Quantum Chem. Symp. 10 (1976) 1.
[9] R. Krishnan, J.A. Pople, Int. J Quantum Chem. 14 (1978) 91.
[10] R.J. Bartlett, D.M. Silver, J. Chem. Phys. 62 (1975) 3258.
[11] R.J. Bartlett, G.D. Purvis, Int. J. Quantum Chem. 14 (1978) 561.
[12] W.J. Hehre, R. Ditchfield, J.A. Pople, J. Chem. Phys. 56 (1972) 2257.
[13] P.C. Hariharan, J.A. Pople, Theor. Chim. Acta 28 (1973) 213.
[14] G.W. Spitznagel, T. Clark, J. Chandrasekhar, P.v.R. Schleyer, J. Comput. Chem. 3 (1983) 3633.
[15] T. Clark, J. Chandrasekhar, G.W. Spitznagel, P.v.R. Schleyer, J. Comput. Chem. 4 (1984) 294.
[16] J.E. Del Bene, Hydrogen Bonding: 1, in: P.v.R. Schleyer, N.L. Allinger, T. Clark, J. Gasteiger, P.A. Kollman, H.F. Schaefer III, P.R. Schreiner (Eds.), The Encyclopedia of Computational Chemistry, vol. 2, Wiley, Chichester, UK, 1998, p. 1263.
[17] T.H. Dunning Jr, J. Chem. Phys. 90 (1989) 1007.
[18] R.A. Kendall, T.H. Dunning Jr, R.J. Harrison, J. Chem. Phys. 96 (1992) 6796.
[19] D.E. Woon, T.H. Dunning Jr, J. Chem. Phys. 98 (1993) 1358.
[20] M.J. Frisch, G.W. Trucks, H.B. Schlegel, G.E. Scuseria, M.A. Robb, J.R. Cheeseman, V.G. Zakrzewski, J.A. Montgomery Jr., R.E. Stratmann, J.C. Burant, S. Dapprich, J.M. Millam, A.D. Daniels, K.N. Kudin, M.C. Strain, O. Farkas, J. Tomasi, V. Barone, M. Cossi, R. Cammi, B. Mennucci, C. Pomelli, C. Adamo, S. Clifford, J. Ochterski, G.A. Petersson, P.Y. Ayala, J. Cui, K. Morokuma, D.K. Malick, A.D. Rabuck, K. Raghavachari, J.B. Foresman, J. Cioslowski, J.V. Ortiz, A.G.

Baboul, B.B. Stefanov, G. Liu, A. Liashenko, P. Piskorz, I. Komaromi, R. Gomperts, R.L. Martin, D.J. Fox, T. Keith, M.A. Al-Laham, C.Y. Peng, A. Nanayakkara, C. Gonzalez, M. Challacombe, P.M.W. Gill, B. Johnson, W. Chen, M.W. Wong, J.L. Andres, C. Gonzalez, M. Head-Gordon, E.S. Replogle, J.A. Pople, GAUSSIAN-98, Gaussian Inc., Pittsburgh, PA, 1998.

[21] T.M. Becker, K. Jayasimhulu, M. Orchin, J. Organomet. Chem. 610 (2000) 118.

[22] G.Q. Li, R.M. Burns, S.K. Mandal, J. Krause Bauer, M. Orchin, J. Organomet. Chem. 549 (1997) 89.

[23] G.Q. Li, J. Feldman, J.A. Krause, M. Orchin, Polyhedron 16 (1997) 2041.

[24] T.M. Becker, J.A. Krause Bauer, M. Orchin, Unpublished results.

[25] A Cambridge Structural Database Search (version 2.3.8) revealed that the majority of Group 6–8 first and second row transition metal M–F bonds occur below 2.00Δ, however, when the F is involved in a bridging motif bonds lengths of 2.00–2.30Δ are observed.

[26] V.J. Murphy, T. Hascall, J.Y. Chen, G. Parkin, J. Am. Chem. Soc. 118 (1996) 7428.

[27] M.K. Whittlesey, R.M. Perutz, B. Greener, M.H. Moore, J. Chem. Soc. Chem. Commun. (1997) 187.

[28] T.M. Becker, J.A. Krause Bauer, Acta Cryst. Sect. C 55 (1999) IUC9900141.

[29] T. Steiner, Acta Cryst. Sect. B 54 (1998) 456.